

CHAPTER 8

SHAPE DESIGN SENSITIVITY ANALYSIS OF NONLINEAR STRUCTURAL SYSTEMS

Nam Ho Kim

*Department of Mechanical and Aerospace Engineering
University of Florida, P.O. Box 116250
Gainesville, Florida 32611, USA
E-mail: nkim@ufl.edu*

Recent developments in design sensitivity analysis of nonlinear structural systems are presented. Various aspects, such as geometric, material, and boundary nonlinearities are considered. The idea of variation in continuum mechanics is utilized in differentiating the nonlinear equations with respect to design variables. Due to the similarity between variation in design sensitivity analysis and linearization in nonlinear analysis, the same tangent stiffness is used for both sensitivity and structural analyses. It has been shown that the computational cost of sensitivity calculation is a small fraction of the structural analysis cost. Such efficiency is due to the fact that sensitivity analysis does not require convergence iteration and it uses the same tangent stiffness matrix with structural analysis. Two examples are presented to demonstrate the accuracy and efficiency of the proposed sensitivity calculation method in nonlinear problems.

1. Introduction

Engineering design often takes into account the nonlinear behavior of the system, such as the design of a metal forming process and the crashworthiness of a vehicle. Nonlinearities in structural problems include material, geometric, and boundary nonlinearities.¹ Geometric nonlinearity occurs when the structure experiences large deformation and is described using the material or spatial formulation. Material nonlinearity is caused by the nonlinear relationship between stress and strain and includes nonlinear elasticity, hyperelasticity, elastoplasticity, etc. A contact/impact problem is often called a boundary nonlinearity, categorized by flexible-rigid and multibody contact/impact conditions. These nonlinearities are often combined together in many structural applications. In the sheet metal forming process,² for example, the blank material

will experience contact with the punch and die (boundary nonlinearity), through which the blank material will be deformed to a desired shape (geometric nonlinearity). At the same time, the blank material will experience permanent, plastic deformation (material nonlinearity).

Design sensitivity analysis^{3,4} of nonlinear structures concerns the relationship between design variables available to the design engineers and performance measure determined through the nonlinear structural analysis. We use the term “design sensitivity” in order to distinguish it from parameter sensitivity. The performance measures include: the weight, stiffness, and compliance of the structure; the fatigue life of a mechanical component; the noise in the passenger compartment of the automobile; the vibration of a beam or plate; the safety of a vehicle in a crash, etc. Any system parameters that the design engineers can change can serve as design variables, including the cross-sectional geometry of beams, the thickness of plates, the shape of parts, and the material properties.

Design sensitivity analysis can be thought of as a variation of the performance measure with respect to the design variable.⁵ Most literature in design sensitivity analysis focuses on the first-order variation, which is similar to the linearization process. In that regard, sensitivity analysis is inherently linear. The recent development of second-order sensitivity analysis also uses a series of linear design sensitivity analyses in order to calculate the second-order variation.^{6,7}

Different methods of sensitivity calculation have been developed in the literature, including global finite differences,^{8,9} continuum derivatives,¹⁰⁻¹² discrete derivatives,¹³⁻¹⁵ and automatic differentiation.¹⁶⁻¹⁸ The global finite difference method is the easiest way to calculate sensitivity information, and repeatedly evaluates the performance measures at different values of the design variables. Engineering problems are often approximated using various numerical techniques, such as the finite element method. The continuum equation is approximated by a discrete system of equations. The discrete derivatives can be obtained by differentiating the discrete system of equations. The continuum derivatives use the idea of variation in continuum mechanics to evaluate the first-order variation of the performance function. After the continuum form of the design sensitivity equation is obtained, a numerical approximation, such as the finite element method, can be used to solve the sensitivity equation. The difference between discrete and continuum derivatives is the order between differentiation and discretization. Finally, automatic differentiation refers to a differentiation of the computer code itself by defining the derivatives of elementary functions, which propagate through complex functions using the chain rule of differentiation. The accuracy, efficiency, and implementation efforts of these methods are discussed by van Keulen *et al.*¹⁹

In this text, only the continuum derivatives are considered, assuming that the same idea can be implemented to the discrete derivatives. In the finite difference and computational differentiation, there is no need to distinguish linear and nonlinear problems, as these two approaches are identical for both problems.

In spite of the rigorous development of the existence and uniqueness of design sensitivity in linear systems,²⁰ no literature is available regarding existence and uniqueness of design sensitivity in nonlinear problems. In this text, the relation between design variables and the performance measures is assumed to be continuous and differentiable. However, by no means should this important issue in differentiability be underestimated.

The organization of the text is as follows. In Section 2, the design sensitivity formulation of nonlinear elastic problems is presented. The unique property of the problems in this category is that the sensitivity equation needs to be solved once at the end of the converged configuration. Thus, the sensitivity calculation is extremely inexpensive; basically, it is the same as that of linear problems.

In Section 3, the design sensitivity formulation of elastoplastic problems is presented. Because the constitutive relation is given as a rate form and the problem at hand is history-dependent, the sensitivity equation needs to be solved at each load step. However, the sensitivity calculation is still inexpensive compared with the nonlinear structural analysis, because the convergence iteration is not required in the sensitivity calculation. After the convergence iteration is finished, the linear sensitivity equation is solved using the decomposed coefficient matrix from the structural analysis.

In Section 4, the design sensitivity formulation of contact problems is presented. The penalty-regularized variational equation is differentiated with respect to design variables.

This chapter is by no means comprehensive in terms of deriving sensitivity formulations. The reader interested in detailed derivations is referred to the literature.²¹⁻²⁹

2. Design Sensitivity Analysis of Nonlinear Elastic Problems

When the deformation of a structure is significant, the initial (undeformed) domain (Ω_X) is distinguished from the deformed domain (Ω_x). A material point $\mathbf{X} \in \Omega_X$ is deformed to a point $\mathbf{x} \in \Omega_x$, such that $\mathbf{x}(\mathbf{X}) = \mathbf{X} + \mathbf{z}(\mathbf{X})$, with $\mathbf{z}(\mathbf{X})$ being the displacement (see Fig. 1).

The weak form of a static problem, whether it is elastic or elastoplastic, can be stated that to find the solution $\mathbf{z} \in \mathcal{V}$, such that

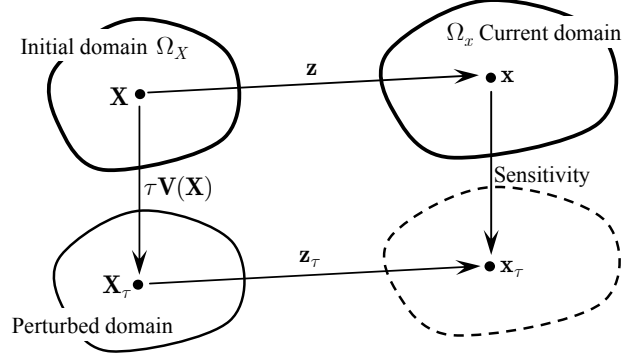


Figure 1. Illustration of shape design perturbation in a nonlinear structural problem. The initial domain is deformed to the current domain. For a given shape design variable, the design velocity field $\mathbf{V}(\mathbf{X})$ is defined in the initial domain. Design sensitivity analysis is then to estimate the deformation of the perturbed domain without actually performing additional nonlinear analysis.

$$a_{\Omega}(\mathbf{z}, \bar{\mathbf{z}}) = \ell_{\Omega}(\bar{\mathbf{z}}), \quad (1)$$

for all $\bar{\mathbf{z}} \in \mathbb{Z}$. In Eq. (1), \mathcal{V} is the solution space and \mathbb{Z} is the space of kinematically admissible displacements. $a_{\Omega}(\mathbf{z}, \bar{\mathbf{z}})$ and $\ell_{\Omega}(\bar{\mathbf{z}})$ are the energy and load forms, respectively, whose expressions depend on the formulations. In many cases, the load form is simple and often it is independent of the deformation. Thus, emphasis will be given to the energy form.

In nonlinear structural analysis, two approaches have been introduced: the total and the updated Lagrangian formulations.¹ The former refers to Ω_X as a reference, whereas the latter uses Ω_x as a reference. In both formulations, equilibrium equations are obtained using the principle of virtual work. These equations are then linearized to yield the incremental form. As noted by Bathe¹, these two formulations are analytically equivalent.

2.1. Total Lagrangian Formulation

2.1.1. Incremental Solution Procedure

When Ω_X is the reference, the energy form in Eq. (1) can be written as

$$a_{\Omega_X}(\mathbf{z}, \bar{\mathbf{z}}) = \iint_{\Omega_X} \mathbf{S}(\mathbf{z}) : \mathbf{E}(\mathbf{z}; \bar{\mathbf{z}}) d\Omega_X, \quad (2)$$

where $\mathbf{S}(\mathbf{z})$ is the second Piola–Kirchhoff stress tensor, ‘:’ is the double contraction operator, and $\mathbf{E}(\mathbf{z}; \bar{\mathbf{z}})$ is the variation of the Green–Lagrange strain tensor, whose expression is given as

$$\mathbf{E}(\mathbf{z}; \bar{\mathbf{z}}) = \text{sym}(\nabla_0 \bar{\mathbf{z}}^T \cdot \mathbf{F}), \quad (3)$$

where $\text{sym}(\mathbf{A}) = \frac{1}{2}(\mathbf{A} + \mathbf{A}^T)$ represents the symmetric part of a tensor, $\mathbf{F} = \nabla_0 \mathbf{x}$ is the deformation gradient, and $\nabla_0 = \partial / \partial \mathbf{X}$ is the gradient operator in the initial domain. Note that $\mathbf{E}(\mathbf{z}; \bullet)$ is linear with respect to its argument, while $\mathbf{S}(\mathbf{z})$ is generally nonlinear.

The load form is independent of the deformation, and is defined as

$$\ell_{\Omega_X}(\bar{\mathbf{z}}) = \iint_{\Omega_X} \bar{\mathbf{z}}^T \cdot \mathbf{f}^B d\Omega + \int_{\Gamma_X^S} \bar{\mathbf{z}}^T \cdot \mathbf{f}^S d\Gamma, \quad (4)$$

where \mathbf{f}^B is the body force and \mathbf{f}^S the surface traction on the boundary Γ_X^S . The deformation-dependent load form can be found in Schweizerhof.³⁰

Since the energy form is nonlinear, an incremental solution procedure, such as the Newton-Raphson method, is often employed through linearization. Let $\mathbb{L}[\bullet]$ denote the linearization operator with respect to incremental displacement $\Delta \mathbf{z}$. Then the energy form in Eq. (2) can be linearized, as

$$\begin{aligned} \mathbb{L}[a_{\Omega_X}(\mathbf{z}, \bar{\mathbf{z}})] &= \iint_{\Omega_X} [\mathbf{E}(\mathbf{z}; \bar{\mathbf{z}}) : \mathbf{C} : \mathbf{E}(\mathbf{z}; \Delta \mathbf{z}) + \mathbf{S}(\mathbf{z}) : \mathbf{H}(\Delta \mathbf{z}, \bar{\mathbf{z}})] d\Omega_X \\ &\equiv a_{\Omega_X}^*(\mathbf{z}; \Delta \mathbf{z}, \bar{\mathbf{z}}), \end{aligned} \quad (5)$$

where \mathbf{C} is the material tangent moduli, obtained from $\mathbb{L}[\mathbf{S}(\mathbf{z})] = \mathbf{C} : \mathbf{E}(\mathbf{z}; \Delta \mathbf{z})$, and the increment of $\mathbf{E}(\mathbf{z}; \bar{\mathbf{z}})$ is given as

$$\mathbf{H}(\Delta \mathbf{z}, \bar{\mathbf{z}}) = \text{sym}(\nabla_0 \bar{\mathbf{z}}^T \cdot \nabla_0 \Delta \mathbf{z}). \quad (6)$$

The notation of $a_{\Omega_X}^*(\mathbf{z}; \Delta \mathbf{z}, \bar{\mathbf{z}})$ is selected such that it implicitly depends on the total displacement \mathbf{z} , and has two parameters $\Delta \mathbf{z}$ and $\bar{\mathbf{z}}$. Note that $a_{\Omega_X}^*(\mathbf{z}; \bullet, \bullet)$ is bilinear and symmetric with respect to its two arguments.

In the solution procedure of a nonlinear problem, the applied load is divided by N load steps and a convergence iteration is carried out at each load step. Let the left superscript n denote the current load step and the right superscript k the iteration counter. Then, the incremental equation can be written as

$$a_{\Omega_X}^*({}^n \mathbf{z}^k; \Delta \mathbf{z}^k, \bar{\mathbf{z}}) = \ell_{\Omega_X}^n(\bar{\mathbf{z}}) - a_{\Omega_X}({}^n \mathbf{z}^k, \bar{\mathbf{z}}), \quad (7)$$

for all $\bar{\mathbf{z}} \in \mathbb{Z}$. $\ell_{\Omega_X}^n(\bar{\mathbf{z}})$ is the load form at the current load step. After solving the incremental displacement $\Delta \mathbf{z}^k$, the total displacement is updated using ${}^n \mathbf{z}^{k+1} = {}^n \mathbf{z}^k + \Delta \mathbf{z}^k$. The iteration in Eq. (7) is repeated until the right-hand side (residual term) vanishes. After the solution is converged, the load step is increased. This procedure is repeated until the last load step N .

Note that Eq. (7) is still in the continuum form, and the discretization is not introduced yet. If the finite element method is used to approximate Eq. (7), the discrete counter part will be

$$[{}^n\mathbf{K}^k]\{\Delta\mathbf{U}^k\} = \{{}^n\mathbf{R}^k\}, \quad (8)$$

where $[{}^n\mathbf{K}^k]$ is the tangent stiffness matrix, $\{\Delta\mathbf{U}^k\}$ the vector of incremental nodal displacements, and $\{{}^n\mathbf{R}^k\}$ the vector of residual forces.

2.1.2. Shape Sensitivity Formulation

A shape design variable is defined in order to change the geometry of the structure. The concept of design velocity is often used for this purpose, which represents the direction of design change for a given shape design variable. By introducing a scalar parameter τ that can control the magnitude of the design change, the perturbed design, as shown in Fig. 1, in the direction of the design velocity can be obtained as

$$\mathbf{X}_\tau = \mathbf{X} + \tau\mathbf{V}(\mathbf{X}). \quad (9)$$

The perturbation process in Eq. (9) is similar to the dynamic process by considering τ as time. Because of this analogy, the direction $\mathbf{V}(\mathbf{X})$ of the design change is called the design velocity.

For a given design velocity, the sensitivity of a function is defined as a material derivative with respect to the parameter τ . For example, the material derivative of displacement can be written as

$$\dot{\mathbf{z}} \equiv \left. \frac{d}{d\tau} [\mathbf{z}_\tau(\mathbf{X}_\tau)] \right|_{\tau=0} = \lim_{\tau \rightarrow 0} \frac{\mathbf{z}_\tau(\mathbf{X}_\tau) - \mathbf{z}(\mathbf{X})}{\tau}. \quad (10)$$

As in continuum mechanics, the above material derivative can be decomposed by the partial derivative and the convective term, as

$$\dot{\mathbf{z}}(\mathbf{X}) = \mathbf{z}'(\mathbf{X}) + \nabla_0\mathbf{z} \cdot \mathbf{V}(\mathbf{X}). \quad (11)$$

Even if the partial derivative is interchangeable with the spatial gradient, the material derivative is not.³ The following relation should be used for the material derivative of the spatial gradient:

$$\left. \frac{d}{d\tau} (\nabla_0\mathbf{z}) \right|_{\tau=0} = \nabla_0\dot{\mathbf{z}} - \nabla_0\mathbf{z} \cdot \nabla_0\mathbf{V}. \quad (12)$$

Since stress and strain include the gradient of the displacement, their material derivative will include the unknown term $\nabla_0\dot{\mathbf{z}}$ (implicit dependence) and the known term $\nabla_0\mathbf{z} \cdot \nabla_0\mathbf{V}$ (explicit dependence). The design sensitivity analysis solves for the first using the second. For example, the material derivative of the strain variation in Eq. (3) can be written as

$$\left. \frac{d}{d\tau} \mathbf{E}(\mathbf{z}; \bar{\mathbf{z}}) \right|_{\tau=0} = \mathbf{H}(\dot{\mathbf{z}}; \bar{\mathbf{z}}) + \mathbf{H}_V(\mathbf{z}; \bar{\mathbf{z}}), \quad (13)$$

with the explicitly dependent term being

$$\mathbf{H}_V(\mathbf{z}; \bar{\mathbf{z}}) = -sym[(\nabla_0 \bar{\mathbf{z}} \cdot \nabla_0 \mathbf{V})^T \cdot \mathbf{F}] - sym[\nabla_0 \bar{\mathbf{z}}^T \cdot (\nabla_0 \mathbf{z} \cdot \nabla_0 \mathbf{V})]. \quad (14)$$

Let the incremental equation (7) be converged at the last load step, which means that the nonlinear variational equation (1) is satisfied. Then, Eq. (1) is differentiated with respect to the parameters τ to obtain the following design sensitivity equation:

$$a_{\Omega_X}^*(\mathbf{z}; \dot{\mathbf{z}}, \bar{\mathbf{z}}) = \ell'_V(\bar{\mathbf{z}}) - a'_V(\mathbf{z}, \bar{\mathbf{z}}), \quad (15)$$

for all $\bar{\mathbf{z}} \in \mathcal{Z}$. The first term on the right-hand side is the explicit term from the load form and the second from the energy form. These explicit terms can be obtained after differentiating with respect to parameter τ , as

$$\begin{aligned} \ell'_V(\bar{\mathbf{z}}) &= \iint_{\Omega_X} \bar{\mathbf{z}}^T \cdot [(\nabla_0 \mathbf{f}^B \cdot \mathbf{V}) + \mathbf{f}^B div \mathbf{V}] d\Omega \\ &+ \int_{\Gamma_X^S} \bar{\mathbf{z}}^T \cdot [(\nabla_0 \mathbf{f}^S \cdot \mathbf{V}) + \kappa \mathbf{f}^B (\mathbf{V} \cdot \mathbf{N})] d\Gamma \end{aligned} \quad (16)$$

and

$$a'_V(\mathbf{z}, \bar{\mathbf{z}}) = \iint_{\Omega_X} [\mathbf{E}(\mathbf{z}; \bar{\mathbf{z}}) : \mathbf{C} : \mathbf{E}_V(\mathbf{z}) + \mathbf{S} : \mathbf{H}_V(\mathbf{z}; \bar{\mathbf{z}}) + \mathbf{S} : \mathbf{E}(\mathbf{z}; \bar{\mathbf{z}}) div \mathbf{V}] d\Omega, \quad (17)$$

where $div \mathbf{V}$ is the divergence of the design velocity, and

$$\mathbf{E}_V(\mathbf{z}) = -sym[(\nabla_0 \mathbf{z} \cdot \nabla_0 \mathbf{V}) \cdot \mathbf{F}] \quad (18)$$

is the explicitly dependent term from the Green–Lagrange strain. In Eq. (16), κ is the curvature of the boundary, and \mathbf{N} the unit normal vector to the boundary.

The design sensitivity equation (15) in continuum form can be discretized using the same method with the nonlinear structural analysis. We assume that the nonlinear problem has been solved up to the final load step N and the final iteration K . If the finite element method is used to approximate Eq. (15), the discrete form of the sensitivity equation will be

$$[{}^N \mathbf{K}^K] \{\dot{\mathbf{U}}\} = \{\mathbf{R}^{fic}\}, \quad (19)$$

where $[{}^N \mathbf{K}^K]$ is the tangent stiffness matrix at the last analysis, which is already factorized from the structural analysis; $\{\dot{\mathbf{U}}\}$ the vector of nodal displacement sensitivity; and $\{\mathbf{R}^{fic}\}$ the fictitious load representing the right-hand side of Eq. (15).

If Eq. (7) is compared with Eq. (15), the left-hand sides are identical except that the former solves for $\Delta \mathbf{z}$, while the latter for $\dot{\mathbf{z}}$. The computational advantage of sensitivity analysis comes from the fact that the linear equation (15) is solved once at the last converged load step. In addition, the LU-decomposed

tangent stiffness matrix can be used in solving for $\dot{\mathbf{z}}$ with a different right-hand side, often called the fictitious load³ or the pseudo load.¹¹

If $a_{\Omega_X}^*(\mathbf{z}; \Delta\mathbf{z}, \bar{\mathbf{z}})$ is a true linearization of $a_{\Omega_X}(\mathbf{z}, \bar{\mathbf{z}})$, this method provides a quadratic convergence when the initial estimate is close to the solution. Even if the tangent operator is inexact, the structural analysis may still converge after a greater number of iterations are performed. However, in sensitivity analysis the inexact tangent operator produces an error in the sensitivity result because no iteration is involved. Without accurate tangent stiffness, sensitivity iteration is required,³¹ which significantly reduces the efficiency of sensitivity calculation.

In shape sensitivity analysis, the total Lagrangian formulation has been more popular than the updated Lagrangian formulation.³²⁻³⁵ This is partly because the reference configuration Ω_X is the same as the design reference. However, it will be shown in the next section that the sensitivity expressions of the two formulations are identical after appropriate transformation.

2.2. Updated Lagrangian Formulation

2.2.1. Incremental Solution Procedure

The updated Lagrangian formulation uses Ω_x as a reference. The energy form in the updated Lagrangian formulation can be written as

$$a_{\Omega_x}(\mathbf{z}, \bar{\mathbf{z}}) = \iint_{\Omega_x} \boldsymbol{\sigma}(\mathbf{z}) : \boldsymbol{\varepsilon}(\bar{\mathbf{z}}) d\Omega, \quad (20)$$

where $\boldsymbol{\sigma}(\mathbf{z})$ is the Cauchy stress tensor, $\boldsymbol{\varepsilon}(\bar{\mathbf{z}})$ the variation of the engineering strain tensor, whose expression is given as

$$\boldsymbol{\varepsilon}(\bar{\mathbf{z}}) = \text{sym}(\nabla_x \bar{\mathbf{z}}), \quad (21)$$

and $\nabla_x = \partial / \partial \mathbf{x}$ is the spatial gradient operator. The same load form in the total Lagrangian formulation is used.³⁶

Even if Eqs. (2) and (20) seem different, it is possible to show that they are identical using the following relations:

$$\boldsymbol{\varepsilon}(\bar{\mathbf{z}}) = \mathbf{F}^{-T} \cdot \mathbf{E}(\mathbf{z}; \bar{\mathbf{z}}) \cdot \mathbf{F}^{-1}, \quad (22)$$

$$\boldsymbol{\sigma}(\mathbf{z}) = \frac{1}{J} \mathbf{F} \cdot \mathbf{S} \cdot \mathbf{F}^T. \quad (23)$$

The same transformation as in Eq. (22) can be applied for $\mathbf{E}(\mathbf{z}; \Delta\mathbf{z})$. In Eq. (23), J is the Jacobian of the deformation, such that $d\Omega_x = Jd\Omega_X$.

The linearization of Eq. (20) is complicated because not only the stress and strain, but also the domain Ω_x depends on the deformation. Thus, instead of

directly linearizing Eq. (20), it is first transferred to the undeformed configuration (pull-back). After linearization, the incremental form (the same as Eq. (5)) is transferred to the deformed configuration (push-forward) to obtain

$$a_{\Omega_x}^*(\mathbf{z}; \Delta \mathbf{z}, \bar{\mathbf{z}}) \equiv \iint_{\Omega_x} [\boldsymbol{\varepsilon}(\bar{\mathbf{z}}) : \mathbf{c} : \boldsymbol{\varepsilon}(\Delta \mathbf{z}) + \boldsymbol{\sigma}(\mathbf{z}) : \boldsymbol{\eta}(\Delta \mathbf{z}, \bar{\mathbf{z}})] d\Omega, \quad (24)$$

where $c_{ijkl} = F_{iI}F_{jJ}F_{kK}F_{lL}C_{IJKL}$ is the spatial tangent moduli³⁷ and

$$\boldsymbol{\eta}(\Delta \mathbf{z}, \bar{\mathbf{z}}) = \text{sym}(\nabla_x \bar{\mathbf{z}}^T \cdot \nabla_x \Delta \mathbf{z}) \quad (25)$$

is the transformation of $\mathbf{H}(\Delta \mathbf{z}, \bar{\mathbf{z}})$ in Eq. (6).

The same incremental equation as in Eq. (7) can be used for the Newton-Raphson iterative solution procedure with different definitions of $a_{\Omega_x}(\mathbf{z}, \bar{\mathbf{z}})$ and $a_{\Omega_x}^*(\mathbf{z}; \Delta \mathbf{z}, \bar{\mathbf{z}})$. There is one difficulty in the expression of Eq. (20): the reference Ω_x is unknown. For computational convenience, the domain at the previous iteration is often chosen as a reference domain, assuming that as the solution converges, the difference between the two domains can be ignored.

2.2.2. Shape Sensitivity Formulation

From the viewpoint of the shape design, the sensitivity formulation of the updated Lagrangian can be done in two ways: either differentiating the energy form in Eq. (20) directly, or differentiating the total Lagrangian form first and then transforming it to the current configuration. The first is relatively complex because the reference Ω_x depends on both the design and the deformation. Cho and Choi³⁸ differentiate the energy form in Ω_x . Since the design velocity $\mathbf{V}(\mathbf{X})$ is always defined in Ω_X , they update the design velocity at each load step, which requires additional steps in the sensitivity calculation. In addition, this approach cannot take advantage of the computational efficiency, because the sensitivity equation must be solved at each load step.

From the idea that the total and updated Lagrangian formulations are equivalent, the second approach is taken; i.e., transforming the sensitivity Eq. (15) to the deformed configuration to obtain

$$a_{\Omega_x}^*(\mathbf{z}; \dot{\mathbf{z}}, \bar{\mathbf{z}}) = \ell'_V(\bar{\mathbf{z}}) - a'_V(\mathbf{z}, \bar{\mathbf{z}}), \quad (26)$$

for all $\bar{\mathbf{z}} \in \mathbb{Z}$. In Eq. (26), the same $\ell'_V(\bar{\mathbf{z}})$ in Eq. (16) is used, since the difference between two formulations is in the energy form, not in the load form. The explicitly dependent term from the energy form can be obtained, after transformation, as

$$a'_V(\mathbf{z}, \bar{\mathbf{z}}) = \iint_{\Omega_x} [\boldsymbol{\varepsilon}(\bar{\mathbf{z}}) : \mathbf{c} : \boldsymbol{\varepsilon}_V(\mathbf{z}) + \boldsymbol{\sigma} : \boldsymbol{\eta}_V(\mathbf{z}, \bar{\mathbf{z}}) + \boldsymbol{\sigma} : \boldsymbol{\varepsilon}(\bar{\mathbf{z}}) \text{div} \mathbf{V}] d\Omega, \quad (27)$$

where

$$\epsilon_V(\mathbf{z}) = -\text{sym}(\nabla_0 \mathbf{z} \cdot \nabla_x \mathbf{V}), \quad (28)$$

$$\eta_V(\mathbf{z}, \bar{\mathbf{z}}) = -\text{sym}[\nabla_n \bar{\mathbf{z}}^T \cdot (\nabla_0 \mathbf{z} \cdot \nabla_x \mathbf{V})] - \text{sym}[\nabla_0 \bar{\mathbf{z}} \cdot \nabla_x \mathbf{V}]. \quad (29)$$

Note that the sensitivity Eq. (26) solves for the sensitivity of the total displacement, not its increment. Thus, the same efficiency as with the total Lagrangian approach can be expected.

3. Design Sensitivity Analysis of Elastoplastic Problems

In addition to the nonlinear elastic material in the previous section, the elastoplastic material is important in engineering applications. The major difference is that the former has a potential function so that the stress can be determined as a function of state, whereas the latter depends on the load history. In that regard, the elastoplastic problem is often called history-dependent. One of the main disadvantages of this type of problem is that the sensitivity analysis must follow the nonlinear analysis procedure closely.³⁹⁻⁴³ Two formulations are discussed in this section: the rate form and the total form.

3.1. Small Deformation Elastoplasticity

3.1.1. Incremental Solution Procedure

When deformation is small (i.e., infinitesimal), the constitutive relation of elastoplasticity can be given in the rate form, and stress can be additively decomposed into elastic and plastic parts. The elastic part is described using the traditional linear elasticity, while the plastic part (permanent deformation) is described by the evolution of internal plastic variables.

Due to the assumption of small deformation, it is unnecessary to distinguish the deformed configuration from the undeformed one. Since the problem depends on the path of the load, it is discretized by N load steps: $[t_0, t_1, \dots, t_N]$ with the current load step being t_n . In order to simplify the presentation, only isotropic hardening is considered in the following derivations, in which the plastic variable is identical to the effective plastic strain, e_p .

Let the incremental solution procedure converge at load step t_{n-1} and the history-dependent variable ${}^{n-1}\boldsymbol{\xi} = \{{}^{n-1}\boldsymbol{\sigma}, {}^{n-1}e_p\}$ be available. Then, the energy form at t_n can be written as

$$a_\Omega({}^{n-1}\boldsymbol{\xi}; {}^n \mathbf{z}, \bar{\mathbf{z}}) = \iint_\Omega \epsilon(\bar{\mathbf{z}}) : {}^n \boldsymbol{\sigma} \, d\Omega. \quad (30)$$

In Eq. (30), the left superscripts n and $n-1$ represent the load steps t_n and t_{n-1} , respectively. However, they will often be omitted whenever there is no confusion. The notation of the energy form is selected such that it implicitly depends on the history-dependent variable at the pervious load step.

The energy form is nonlinear with respect to its arguments. In order to linearize the energy form, it is necessary to consider the update procedure of the stress and the plastic variable. In the displacement-driven procedure, it is assumed that the displacement increment $\Delta \mathbf{z}$ is given from the previous iteration. Mathematically, elastoplasticity can be viewed as a projection of stress onto the elastic domain, which can be accomplished using a trial elastic predictor followed by a plastic corrector. Then, the stress and the plastic variable can be updated according to

$${}^n \boldsymbol{\sigma} = {}^{n-1} \boldsymbol{\sigma} + \mathbf{C} : \Delta \boldsymbol{\varepsilon} - 2\mu\gamma \mathbf{N}, \quad (31)$$

$${}^n e_p = {}^{n-1} e_p + \sqrt{\frac{2}{3}} \gamma, \quad (32)$$

where $\mathbf{C} = (\lambda + \frac{2}{3}\mu)\mathbf{1} \otimes \mathbf{1} + 2\mu\mathbf{I}_{dev}$ is the fourth-order isotropic constitutive tensor; λ and μ are Lamé's constants; $\Delta \boldsymbol{\varepsilon} = \boldsymbol{\varepsilon}(\Delta \mathbf{z})$ is the incremental strain; \mathbf{N} is a unit deviatoric tensor, normal to the yield function; and γ is the plastic consistency parameter. In Eq. (31), the first two terms on the right-hand side correspond to the trial stress; i.e., ${}^{tr} \boldsymbol{\sigma} = {}^{n-1} \boldsymbol{\sigma} + \mathbf{C} : \Delta \boldsymbol{\varepsilon}$.

The plastic consistency parameter can be obtained from the relation that the stress stays on the boundary of the yield function during the continuous yielding:

$$f({}^n \mathbf{s}, {}^n e_p) = \|{}^n \mathbf{s}\| - \sqrt{\frac{2}{3}} \kappa({}^n e_p) = 0, \quad (33)$$

where ${}^n \mathbf{s} = \mathbf{I}_{dev} : {}^n \boldsymbol{\sigma}$ is the deviatoric stress tensor, \mathbf{I}_{dev} is the fourth-order unit deviatoric tensor, $\kappa({}^n e_p)$ is the radius of the elastic domain in the isotropic hardening plastic model. In general, the above equation is nonlinear, so that the local Newton-Raphson method can be used for the plastic consistency parameter. When there is no plastic deformation, γ is equal to zero.

Using the update procedure described in Eqs. (31)–(33), the energy form can be linearized to obtain

$$a_{\Omega}^*({}^{n-1} \boldsymbol{\xi}; \Delta \mathbf{z}, \bar{\mathbf{z}}) = \iint_{\Omega} \boldsymbol{\varepsilon}(\bar{\mathbf{z}}) : \mathbf{C}^{alg} : \boldsymbol{\varepsilon}(\Delta \mathbf{z}) d\Omega, \quad (34)$$

where the algorithmic tangent operator⁴⁴ is defined by

$$\mathbf{C}^{alg} = \mathbf{C} - \frac{4\mu^2}{A} \mathbf{N} \otimes \mathbf{N} - \frac{4\mu^2 \gamma}{\|{}^{tr} \mathbf{s}\|} [\mathbf{I}_{dev} - \mathbf{N} \otimes \mathbf{N}], \quad (35)$$

where $A = 2\mu + \frac{2}{3} \partial \kappa / \partial e_p$; \otimes is the tensor product; and ${}^{tr} \mathbf{s}$ is the deviatoric stress at the trial state, which can be obtained by assuming that all incremental

displacements are elastic. To guarantee the quadratic convergence of the nonlinear analysis, the algorithmic tangent operator must be consistent with the stress update algorithm.⁴⁴

Once the energy form and the linearized energy form are available, the same linear equation as Eq. (7) can be used to solve for the incremental displacement. After the residual term vanishes, the stress and the plastic variable are updated according to Eqs. (31) and (32), the analysis moves to the next load step, and proceeds until the last load step.

3.1.2. Shape Sensitivity Formulation

In the shape design sensitivity formulation for the elastoplastic material, it is assumed that the structural problem has been solved up to the load step t_n and the sensitivity analysis has been finished up to the load step t_{n-1} . The goal is to solve the sensitivity equation at the load step t_n . This is necessary because the problem at hand is history-dependent. At each load step, the sensitivity of the incremental displacement is solved, and the sensitivity of the stress and the plastic variable is updated for the sensitivity calculation at the next load step.

By differentiating the variational equation (1) with the energy form in Eq. (30), the sensitivity equation can be obtained as

$$a_{\Omega}^*({}^{n-1}\boldsymbol{\xi}; \Delta \dot{\mathbf{z}}, \bar{\mathbf{z}}) = \ell'_V(\bar{\mathbf{z}}) - a'_V({}^n \mathbf{z}, \bar{\mathbf{z}}) - a'_p({}^{n-1}\boldsymbol{\xi}, {}^n \mathbf{z}, \bar{\mathbf{z}}), \quad (36)$$

for all $\bar{\mathbf{z}} \in \mathbb{Z}$. The linearized energy form $a_{\Omega}^*({}^{n-1}\boldsymbol{\xi}; \bullet, \bullet)$ is identical with that of Eq. (34). Two differences can be observed in the above sensitivity equation compared to the elastic problem: (1) it solves for the sensitivity of incremental displacement $\Delta \dot{\mathbf{z}}$, and (2) it depends on the sensitivity results at the previous load step. In Eq. (36), the explicit term from the load form is similar to Eq. (16), and the explicit term from the energy form is defined as

$$a'_V(\mathbf{z}, \bar{\mathbf{z}}) = \iint_{\Omega} [\boldsymbol{\varepsilon}_V(\bar{\mathbf{z}}) : \boldsymbol{\sigma} + \boldsymbol{\varepsilon}(\bar{\mathbf{z}}) : \mathbf{C}^{\text{alg}} : \boldsymbol{\varepsilon}_V(\mathbf{z}) + \boldsymbol{\varepsilon}(\bar{\mathbf{z}}) : \boldsymbol{\sigma} \text{div} \mathbf{V}] d\Omega, \quad (37)$$

where

$$\boldsymbol{\varepsilon}_V(\mathbf{z}) = -\text{sym}(\nabla \mathbf{z} \cdot \nabla \mathbf{V}) \quad (38)$$

is the explicit term from the material derivative of the strain tensor. The last term in Eq. (36), the history-dependent term, is given as

$$a'_p(\mathbf{z}, \bar{\mathbf{z}}) = \iint_{\Omega} [\boldsymbol{\varepsilon}(\bar{\mathbf{z}}) : \boldsymbol{\sigma}^{\text{fic}}] d\Omega, \quad (39)$$

where

$$\boldsymbol{\sigma}^{fic} = {}^{n-1}\dot{\boldsymbol{\sigma}} - \frac{2\mu}{A} \left[\mathbf{N} : {}^{n-1}\dot{\mathbf{s}} - \sqrt{\frac{2}{3}} \frac{\partial \kappa}{\partial e_p} {}^{n-1}\dot{e}_p \right] \mathbf{N} - \frac{2\mu\gamma}{\|\mathbf{tr} \dot{\mathbf{s}}\|} (\mathbf{I} - \mathbf{N} \otimes \mathbf{N}) : {}^{n-1}\dot{\mathbf{s}} \quad (40)$$

is the plastic variable from the sensitivity calculation at the previous load step.

After the sensitivity equation is solved, the sensitivity of the total displacement can be updated by

$${}^n \dot{\mathbf{z}} = {}^{n-1} \dot{\mathbf{z}} + \Delta \dot{\mathbf{z}}. \quad (41)$$

In addition, the sensitivity of the stress and the plastic variable must be updated for the calculation in the next load step, using the following formulas:

$${}^n \dot{\boldsymbol{\sigma}} = {}^{n-1} \dot{\boldsymbol{\sigma}} + \mathbf{C} : [\boldsymbol{\varepsilon}(\Delta \dot{\mathbf{z}}) + \boldsymbol{\varepsilon}_V(\Delta \dot{\mathbf{z}})], \quad (42)$$

$${}^n \dot{e}_p = {}^{n-1} \dot{e}_p + \frac{1}{A} \sqrt{\frac{2}{3}} \left[\mathbf{N} : {}^n \dot{\mathbf{s}} - \sqrt{\frac{2}{3}} \frac{\partial \kappa}{\partial e_p} {}^{n-1} \dot{e}_p \right]. \quad (43)$$

The fact that the sensitivity equation needs to be solved at each load step may decrease the computational advantage. However, the sensitivity calculation is still inexpensive compared to the structural analysis. First, the convergence iteration in the nonlinear problem is avoided and the linear sensitivity equation is solved at the end of each load step. Second, the LU-decomposed stiffness matrix from structural analysis can be used for sensitivity calculation. Considering the fact that most computational cost in the matrix equation is involved in the decomposition, the proposed sensitivity calculation method provides a significant advantage. The major cost in sensitivity calculation is involved in the construction of the fictitious load and updating the history-dependent variables.

3.2. Finite Deformation Elastoplasticity

When a structure undergoes a large deformation, the elastoplasticity theory with the infinitesimal deformation needs to be modified. A new method for expressing the kinematics of finite deformation elastoplasticity using the hyperelastic constitutive relation is becoming a desirable approach for isotropic material. This method defines a stress-free intermediate configuration composed of plastic deformation, and obtains the stress from the elastic strain energy density function defined in the intermediate configuration (see Fig. 2).

In this model, the deformation gradient is decomposed by the elastic and plastic parts,⁴⁵ as

$$\mathbf{F}(\mathbf{X}) = \mathbf{F}_e(\mathbf{X}) \cdot \mathbf{F}_p(\mathbf{X}), \quad (44)$$

where $\mathbf{F}_p(\mathbf{X})$ is the deformation through the intermediate domain, which is related to the plastic deformation, and \mathbf{F}_e^{-1} is the stress-free, unloaded process.

3.2.1. Incremental Solution Procedure

Similar to the previous section, the load is discretized by N load steps and the current load step is t_n . In order to simplify the presentation, only isotropic hardening is considered in the following derivations. In the incremental solution process, it is assumed that the nonlinear analysis has been converged and plastic variables ${}^{n-1}\boldsymbol{\xi} = \{{}^{n-1}\mathbf{F}_p, {}^{n-1}e_p\}$ are available from load step t_{n-1} .

The variational equation is similar to that of the updated Lagrangian formulation, and the energy form is defined as

$$a_{\Omega_X}({}^{n-1}\boldsymbol{\xi}; {}^n\mathbf{z}, \bar{\mathbf{z}}) = \iint_{\Omega_X} \varepsilon(\bar{\mathbf{z}}) : {}^n\boldsymbol{\tau} d\Omega. \quad (45)$$

Note that the energy form is defined using the integral over domain Ω_X , and the Kirchhoff stress tensor $\boldsymbol{\tau} = J\boldsymbol{\sigma}$ is used so that the effect of Jacobian is included in the constitutive relation.⁴⁶

In order to solve the nonlinear equation (45), the procedure of stress update is presented first. At load step t_n , with given displacement increment, the deformation gradient is calculated by

$${}^n\mathbf{F} = \mathbf{f} \cdot {}^{n-1}\mathbf{F} = {}^{tr}\mathbf{F}_e \cdot {}^{n-1}\mathbf{F}_p, \quad (46)$$

where $\mathbf{f} = \mathbf{1} + \nabla_x \Delta \mathbf{z}$ is the relative deformation gradient, and ${}^{tr}\mathbf{F}_e = \mathbf{f} \cdot {}^{n-1}\mathbf{F}_e$ is

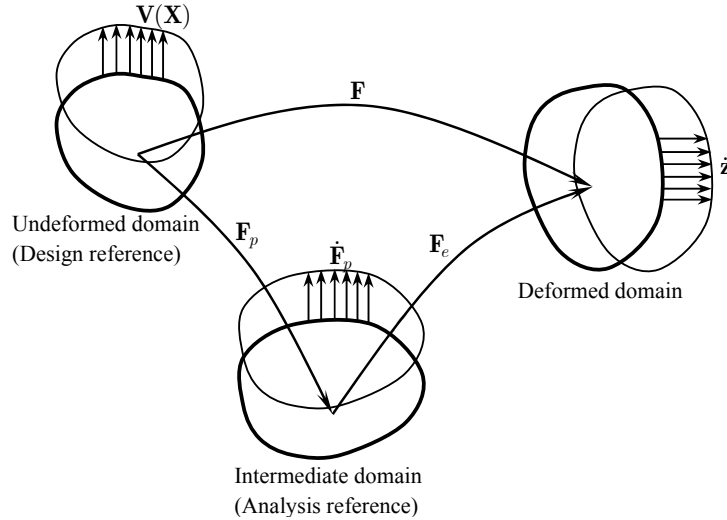


Figure 2. Analysis and design configurations for large deformation elastoplasticity. Plastic deformation is applied to the intermediate domain. The constitutive relation is hyperelasticity between the intermediate and deformed domains. The design velocity is always defined in the undeformed domain.

the trial elastic deformation gradient, which is obtained by assuming that the relative deformation gradient is purely elastic.

Since the trial state assumes that all incremental deformation is elastic, it goes out of the elastic domain when a part of it is plastic deformation. Thus, the trial state needs to return to the elastic domain, which is called the return–mapping. In this model, the return–mapping is achieved in the principal stress space with a fixed principal direction. By using the constitutive relation between the principal stress and logarithmic strain, better accuracy is obtained for a large elastic strain problem than with the classical elastoplasticity.

Let $\mathbf{e} = \{e_1, e_2, e_3\}^T = \{\log(\lambda_1), \log(\lambda_2), \log(\lambda_3)\}^T$ be the logarithmic principal stretch of the elastic left Cauchy–Green deformation tensor, defined by

$${}^{tr}\mathbf{b}^e = {}^{tr}\mathbf{F}_e \cdot {}^{tr}\mathbf{F}_e^T = \sum_{i=1}^3 \lambda_i^2 \mathbf{n}^i \otimes \mathbf{n}^i. \quad (47)$$

Then, the Kirchhoff stress tensor, after plastic deformation, can be calculated by

$$\boldsymbol{\tau} = \sum_{i=1}^3 \tau_i^p \mathbf{n}^i \otimes \mathbf{n}^i, \quad (48)$$

where $\boldsymbol{\tau}^p = \{\tau_1^p, \tau_2^p, \tau_3^p\}$ is the principal Kirchhoff stress. Note that for the isotropic material, $\boldsymbol{\tau}$ and ${}^{tr}\mathbf{b}^e$ share the same principal directions. Equation (48) means that the principal direction is fixed during the plastic deformation, and the principal Kirchhoff stress is updated, including plastic deformation, as

$${}^n\boldsymbol{\tau}^p = \mathbf{c}^e \cdot \mathbf{e} - 2\mu\gamma\mathbf{N}, \quad (49)$$

where $\mathbf{c}^e = (\lambda + \frac{2}{3}\mu)\tilde{\mathbf{1}} \otimes \tilde{\mathbf{1}} + 2\mu\mathbf{1}_{dev}$ is the 3×3 elastic constitutive tensor for the isotropic material; $\tilde{\mathbf{1}} = \{1, 1, 1\}^T$ is the first–order tensor; $\mathbf{1}_{dev} = \mathbf{1} - \frac{1}{3}(\tilde{\mathbf{1}} \otimes \tilde{\mathbf{1}})$ is the second–order deviatoric tensor; \mathbf{N} is a unit vector, normal to the yield function; and γ is the plastic consistency parameter. If Eq. (49) is compared with Eq. (31), two formulations yield a very similar return–mapping procedure. The differences are that Eq. (49) is in the principal stress space, and the logarithmic principal stretch is used instead of the engineering strain tensor.

The plastic consistency parameter can be obtained from the relation that the stress stays on the yield function during the continuous yielding:

$$f({}^n\mathbf{s}, {}^n e_p) = \|{}^n\mathbf{s}\| - \sqrt{\frac{2}{3}}\kappa({}^n e_p) = 0, \quad (50)$$

where ${}^n\mathbf{s} = \mathbf{1}_{dev} : {}^n\boldsymbol{\tau}^p$ is the deviatoric part of ${}^n\boldsymbol{\tau}^p$, and $\kappa({}^n e_p)$ is the radius of the yield surface after plastic deformation.

The linearization of the energy form is similar to that of the updated Lagrangian formulation, except that the integration domain is changed to the undeformed one:

$$a_{\Omega_X}({}^{n-1}\boldsymbol{\xi}, \mathbf{z}; \Delta \mathbf{z}, \bar{\mathbf{z}}) = \iint_{\Omega_X} [\boldsymbol{\varepsilon}(\bar{\mathbf{z}}) : \mathbf{c} : \boldsymbol{\varepsilon}(\Delta \mathbf{z}) + \boldsymbol{\tau} : \boldsymbol{\eta}(\Delta \mathbf{z}, \bar{\mathbf{z}})] d\Omega. \quad (51)$$

The tangent stiffness moduli \mathbf{c} in the above equation must be consistent with the stress update procedure that is explained between Eqs. (46) and (50). The explicit form of \mathbf{c} is available in Simo.⁴⁶

Using the energy form in Eq. (45) and its linearization in Eq. (51), the Newton-Raphson method, similar to Eq. (7), can be employed to solve for the incremental displacement. Once the residual term is converged through iteration, the plastic variables are updated and analysis moves to the next load step.

Different from the classical elastoplasticity, it is not necessary to store stress because, as is clear from Eq. (49), stress can be calculated from hyperelasticity. Instead, the intermediate configuration, which is represented by \mathbf{F}_p or counter part \mathbf{F}_e , is stored for the calculation in the next load step. For that purpose, first the relative plastic deformation gradient is calculated by

$$\mathbf{f}_p = \sum_{i=1}^3 \exp(-\gamma N_i) \mathbf{n}^i \otimes \mathbf{n}^i, \quad (52)$$

from which the elastic part of the deformation gradient is updated by ${}^n\mathbf{F}_e = \mathbf{f}_p \cdot {}^{tr}\mathbf{F}_e$, and the plastic part can be obtained from ${}^n\mathbf{F}_p = {}^n\mathbf{F}_e^{-1} \cdot {}^n\mathbf{F}$. In addition, the effective plastic strain that determines the radius of the yield surface can be updated by

$${}^n e_p = {}^{n-1} e_p + \sqrt{\frac{2}{3}} \gamma. \quad (53)$$

After the plastic variables are updated, the sensitivity analysis is performed at each converged load step.

3.2.2. Shape Sensitivity Formulation

As mentioned before, the reference for the design is always the undeformed configuration. When the references for the design and analysis are different, transformation is involved in sensitivity differentiation. In the case of finite deformation elastoplasticity, functions in the intermediate configuration are transformed to the undeformed configuration (pull-back). After differentiation, they are transformed to the deformed configuration (push-forward) in order to recover the updated Lagrangian formulation.

By differentiating the nonlinear variational equation (45) with shape design, the following sensitivity equation can be obtained:

$$a_{\Omega_X}^*({}^{n-1}\boldsymbol{\xi}, \mathbf{z}; \dot{\mathbf{z}}, \bar{\mathbf{z}}) = \ell'_V(\bar{\mathbf{z}}) - a'_V(\mathbf{z}, \bar{\mathbf{z}}) - a'_p({}^{n-1}\boldsymbol{\xi}; \mathbf{z}, \bar{\mathbf{z}}), \quad (54)$$

where the explicit term from the load form is given in Eq. (16), and the explicit term from the energy form is given by

$$a_V'(\mathbf{z}, \bar{\mathbf{z}}) = \iint_{\Omega_X} [\varepsilon(\bar{\mathbf{z}}) : \mathbf{c} : \varepsilon_V(\mathbf{z}) + \boldsymbol{\tau} : \boldsymbol{\eta}_V(\mathbf{z}, \bar{\mathbf{z}}) + \boldsymbol{\tau} : \varepsilon(\bar{\mathbf{z}}) \text{div} \mathbf{V}] d\Omega. \quad (55)$$

The expressions of $\varepsilon_V(\mathbf{z})$ and $\boldsymbol{\eta}_V(\mathbf{z}, \bar{\mathbf{z}})$ are identical to those in the updated Lagrangian formulation in Sec. 2.2. The last term on the right-hand side of Eq. (54) is the history-dependent term, which is contributed by the plastic deformation, given as

$$a_p'({}^{n-1}\boldsymbol{\xi}, \mathbf{z}, \bar{\mathbf{z}}) = \iint_{\Omega_X} [\varepsilon(\bar{\mathbf{z}}) : \mathbf{c} : \varepsilon_p(\mathbf{z}) + \boldsymbol{\tau} : \boldsymbol{\eta}_p(\mathbf{z}, \bar{\mathbf{z}}) + \boldsymbol{\tau}^{fic} : \varepsilon(\bar{\mathbf{z}})] d\Omega. \quad (56)$$

The first two integrands are related to the material derivative of the intermediate configuration, and are defined as

$$\varepsilon_p(\mathbf{z}) = -\text{sym}(\mathbf{F}_e \cdot \dot{\mathbf{F}}_p \cdot \mathbf{F}^{-1}), \quad (57)$$

$$\boldsymbol{\eta}_p(\mathbf{z}, \bar{\mathbf{z}}) = -\text{sym}(\nabla_x \bar{\mathbf{z}}^T \cdot \mathbf{F}_e \cdot \dot{\mathbf{F}}_p \cdot \mathbf{F}^{-1}). \quad (58)$$

In addition, the last term in Eq. (56) is related to the history-dependent plastic variable,

$$\boldsymbol{\tau}^{fic} = \sum_{i=1}^3 \left[\frac{\partial \tau_i^p}{\partial e_p} {}^{n-1}\dot{e}_p \right] \mathbf{n}^i \otimes \mathbf{n}^i. \quad (59)$$

Note that the sensitivity equation (54) solves for the sensitivity of the total displacement, which is different from the classical elastoplasticity.

After the sensitivity equation is solved for $\dot{\mathbf{z}}$, the sensitivities of history-dependent terms are updated. For that purpose, the sensitivity of the plastic consistency parameter is first obtained as

$$\dot{\gamma} = \frac{1}{A} \left(2\mu \mathbf{N} \cdot \dot{\mathbf{e}} - \frac{\partial \kappa}{\partial e_p} {}^{n-1}\dot{e}_p \right), \quad (60)$$

where $\dot{e}_i = (\mathbf{n}^i \otimes \mathbf{n}^i) : [\varepsilon(\dot{\mathbf{z}}) + \varepsilon_V(\mathbf{z}) + \varepsilon_p(\mathbf{z})]$. Then, the sensitivity of the effective plastic strain is updated by

$${}^n\dot{e}_p = {}^{n-1}\dot{e}_p + \sqrt{\frac{2}{3}} \dot{\gamma}. \quad (61)$$

The sensitivity of the intermediate domain is also history-dependent, and can be updated by

$${}^n\dot{\mathbf{F}}_p = {}^n\mathbf{F}_e^{-1} \cdot {}^n\dot{\mathbf{F}} - {}^n\mathbf{F}_e^{-1} \cdot {}^n\dot{\mathbf{F}}_e \cdot {}^n\mathbf{F}_e^{-1}, \quad (62)$$

where ${}^n\dot{\mathbf{F}} = \nabla_0 \dot{\mathbf{z}} - \nabla_0 \mathbf{z} \cdot \nabla_0 \mathbf{V}$ and ${}^n\dot{\mathbf{F}}_e = \dot{\mathbf{f}}_p \cdot {}^{tr}\mathbf{F}_e + \mathbf{f}_p \cdot {}^{tr}\dot{\mathbf{F}}_e$. In the above equation, the sensitivity of $\dot{\mathbf{f}}_p$ can be obtained by differentiating Eq. (52). After updating the plastic variables, the nonlinear analysis moves to the next load step.

4. Design Sensitivity Analysis of Contact Problems

Contact problems are common and important aspects of mechanical systems. Metal forming, vehicle crashes, projectile penetration, various seal designs, and bushing and gear systems are only a few examples of contact problems. In this section, the contact condition of a 2D flexible body–rigid wall is considered. This problem can easily be extended to 3D flexible-flexible body contact problems, as shown by Kim et al.²⁸

4.1. Contact Problems with the Rigid Surface

Contact between two bodies can be described using the impenetrability condition, which prevents one body from penetrating into another.^{47,48} Figure 3 illustrates a contact condition with a rigid surface in R^2 . A natural coordinate ξ is used to represent the location on a rigid surface. For example, the contact point \mathbf{x}_c corresponds to the natural coordinate ξ_c , so that $\mathbf{x}_c = \mathbf{x}_c(\xi_c)$.

The impenetrability condition can be imposed on the structure by measuring the gap $g_n(\mathbf{x})$ between $\mathbf{x} \in \Gamma_c$ and the rigid surface, as shown in Fig. 3:

$$g_n \equiv (\mathbf{x} - \mathbf{x}_c(\xi_c)) \cdot \mathbf{e}_n(\xi_c) \geq 0, \quad \mathbf{x} \in \Gamma_c, \quad (63)$$

where $\mathbf{e}_n(\xi_c)$ is the unit outward normal vector of the rigid surface. The contact point \mathbf{x}_c that corresponds to body point $\mathbf{x} \in \Gamma_c$ is determined by solving the following nonlinear equation:

$$(\mathbf{x} - \mathbf{x}_c(\xi_c)) \cdot \mathbf{e}_t(\xi_c) = 0, \quad (64)$$

where $\mathbf{e}_t(\xi_c)$ is the unit tangential vector. The contact point $\mathbf{x}_c(\xi_c)$ is the closest projection point of $\mathbf{x} \in \Gamma_c$ onto the rigid surface that satisfies Eq. (64).

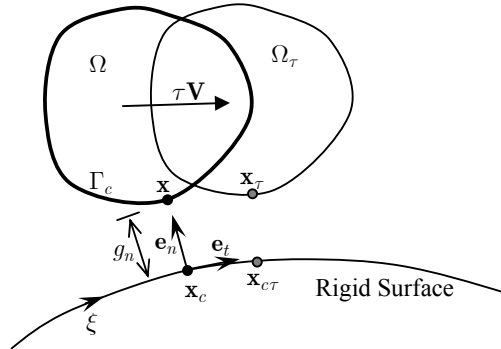


Figure 3. Contact condition between flexible and rigid bodies. The penalty function is established for the region Γ_c where the gap function is less than zero. Shape design change will move the contact point.

The structural problem with the contact condition can be formulated using a variational inequality, which is equivalent to the constrained optimization problem.⁴⁹ In practice, this optimization problem is solved using the penalty method. If there is a region Γ_c that violates Eq. (63), then it is penalized using a penalty function. After applying to the structural problem, the variational equation with the contact condition can be written as

$$a_\Omega(\mathbf{z}, \bar{\mathbf{z}}) + b_\Gamma(\mathbf{z}, \bar{\mathbf{z}}) = \ell_\Omega(\bar{\mathbf{z}}), \quad \forall \bar{\mathbf{z}} \in \mathbb{Z}, \quad (65)$$

where the energy and load forms are identical to the previous sections, depending on the constitutive model. The contact form can be defined from the variation of the penalty function, as

$$b_\Gamma(\mathbf{z}, \bar{\mathbf{z}}) = \omega \int_{\Gamma_c} g_n \bar{\mathbf{z}} \cdot \mathbf{e}_n d\Gamma, \quad (66)$$

where ω is the penalty parameter. In Eq. (66), ωg_n corresponds to the contact force. The nonlinear contact form in Eq. (66) can be linearized to obtain

$$b_\Gamma^*(\mathbf{z}; \Delta \mathbf{z}, \bar{\mathbf{z}}) = \omega \int_{\Gamma_c} \bar{\mathbf{z}} \cdot (\mathbf{e}_n \otimes \mathbf{e}_n) \cdot \Delta \mathbf{z} d\Gamma - \omega \int_{\Gamma_c} \frac{\alpha g_n}{c} \bar{\mathbf{z}} \cdot (\mathbf{e}_t \otimes \mathbf{e}_t) \cdot \Delta \mathbf{z} d\Gamma, \quad (67)$$

where

$$\alpha = \mathbf{e}_n \cdot \mathbf{x}_{c,\xi\xi}, \quad c = \|\mathbf{t}\|^2 - g_n \alpha. \quad (68)$$

Note that there is a component in the tangential direction because of curvature effects. If the rigid surface is approximated by a piecewise linear function, then $\alpha = 0$ and $c = \|\mathbf{t}\|^2$.

Suppose the current load step is t_n and the current iteration count is k . Then, the linearized incremental equation of (65) is obtained as

$$a_\Omega^*({}^n \mathbf{z}^k; \Delta \mathbf{z}^k, \bar{\mathbf{z}}) + b_\Gamma^*({}^n \mathbf{z}^k; \Delta \mathbf{z}^k, \bar{\mathbf{z}}) = \ell_\Omega^n(\bar{\mathbf{z}}) - a_\Omega({}^n \mathbf{z}^k, \bar{\mathbf{z}}) - b_\Gamma({}^n \mathbf{z}^k, \bar{\mathbf{z}}), \quad \forall \bar{\mathbf{z}} \in \mathbb{Z}. \quad (69)$$

The linearized system of (69) is solved iteratively with respect to incremental displacement until the residual forces on the right-hand side vanish at each load step.

4.2. Design Sensitivity Analysis for Contact Problems

The shape design sensitivity formulation of the contact problem has been extensively developed using linear variational inequality.^{50,51} The linear operator theory is not applicable to a nonlinear analysis, and the non-convex property of the constraint set makes it difficult to prove the existence of the derivative. Despite such a lack of mathematical theory, the shape design sensitivity formulation for the contact problem is derived in a general continuum setting. As

a result of the regularizing property of the penalty method, it is assumed that the solution continuously depends on shape design. As has been well established in the literature, differentiability fails in the region where contact status changes.⁵⁰ One good feature of the penalty method is that the contact region is established using a violated region, thus avoiding a non-differentiable region.

It is shown by Kim *et al.*²¹ that the design sensitivity analysis of a frictionless contact problem is path-independent, whereas that of a frictional contact problem is path-dependent and requires information from the previous time step to compute sensitivity at the current time.

In order to derive the derivative of the contact form, the gap function in Eq. (63) is first differentiated with respect to the shape design variable, to obtain

$$\dot{g}_n = (\mathbf{V} + \dot{\mathbf{z}}) \cdot \mathbf{e}_n. \quad (70)$$

In the above derivation, the tangential component has been canceled due to the fact that the perturbed contact point also satisfies the consistency condition. Equation (70) implies that, for an arbitrary perturbation of the structure, only the normal component will contribute to the sensitivity of the gap function.

The contact form in Eq. (66) can then be differentiated with respect to the shape design, as

$$\left. \frac{d}{d\tau} [b_{\Gamma_\tau}(\mathbf{z}_\tau, \bar{\mathbf{z}})] \right|_{\tau=0} = b_\Gamma^*(\mathbf{z}; \dot{\mathbf{z}}, \bar{\mathbf{z}}) + b'_V(\mathbf{z}, \bar{\mathbf{z}}). \quad (71)$$

The first term on the right-hand side represents implicitly dependent terms through $\dot{\mathbf{z}}$, and the second term explicitly depends on \mathbf{V} . The implicit term $b_\Gamma^*(\mathbf{z}; \dot{\mathbf{z}}, \bar{\mathbf{z}})$ is available in Eq. (67) by substituting $\dot{\mathbf{z}}$ into $\Delta\mathbf{z}$. The explicit term $b'_V(\mathbf{z}, \bar{\mathbf{z}})$ is defined as the contact fictitious load and can be obtained by collecting all terms that have explicit dependency on the design velocity, as

$$b'_V(\mathbf{z}, \bar{\mathbf{z}}) = b_\Gamma^*(\mathbf{z}; \mathbf{V}, \bar{\mathbf{z}}) + \omega \int_{\Gamma_c} \kappa g_n \bar{\mathbf{z}} \cdot \mathbf{e}_n V_n d\Gamma. \quad (72)$$

The design sensitivity equation can then be obtained by differentiating the penalty-regularized variational Eq. (65) with respect to the design variable, as

$$a_\Omega^*(\mathbf{z}; \dot{\mathbf{z}}, \bar{\mathbf{z}}) + b_\Gamma^*(\mathbf{z}; \dot{\mathbf{z}}, \bar{\mathbf{z}}) = \ell'_V(\bar{\mathbf{z}}) - a'_V(\mathbf{z}, \bar{\mathbf{z}}) - b'_V(\mathbf{z}, \bar{\mathbf{z}}), \quad \forall \bar{\mathbf{z}} \in \mathbb{Z}. \quad (73)$$

For the frictionless contact problem, the fictitious load of the contact form in Eq. (72) depends on \mathbf{z} and \mathbf{V} . The material derivative formula in Eq. (73) is history-independent. Thus, it is very efficient to compute the design sensitivity of a frictionless contact problem. The design sensitivity equation is solved only once at the last load step with the same tangent stiffness matrix from the structural analysis. As compared with nonlinear response analysis, this property provides great efficiency in the sensitivity computation process.

5. Numerical Examples

5.1. Shape Design Sensitivity Analysis of the Windshield Wiper Problem²⁴

The continuum forms of the structural equation and the sensitivity equation are approximated using the reproducing kernel particle method (RKPM), where the structural domain is represented by a set of particles.^{52,53} RKPM is an ideal choice since, unlike the traditional finite element method, the solution is much less sensitive to the mesh distortion that causes many difficulties in large deformation analysis as well as in shape optimization.

Figure 4(a) shows the geometry of the windshield blade. The windshield is assumed to be a rigid body. For the convenience of the analysis, a vertical line is added to the windshield for smooth deformation. The upper part of the blade is supported by a steel slab. Hyperelastic material (rubber) is used for the blade, and $\omega = 10^7$ is used for the contact penalty.

As the glass moves to the left, the tip of the blade is in contact with the glass, which is modeled as flexible-rigid body contact. The function of the thin neck is to generate flexibility such that the direction of the blade can be easily turned over when the blade changes its moving direction. The role of the wing is to supply enough contact force at the tip point. Figure 4(b) shows a von Mises stress contour plot with the deformed geometry at the final configuration. The stress concentration is found at the neck and the tip because of the bending effect.

The geometry of the structure is parameterized using nine shape design variables as shown in Fig. 4(a). The design velocity at the boundary is obtained

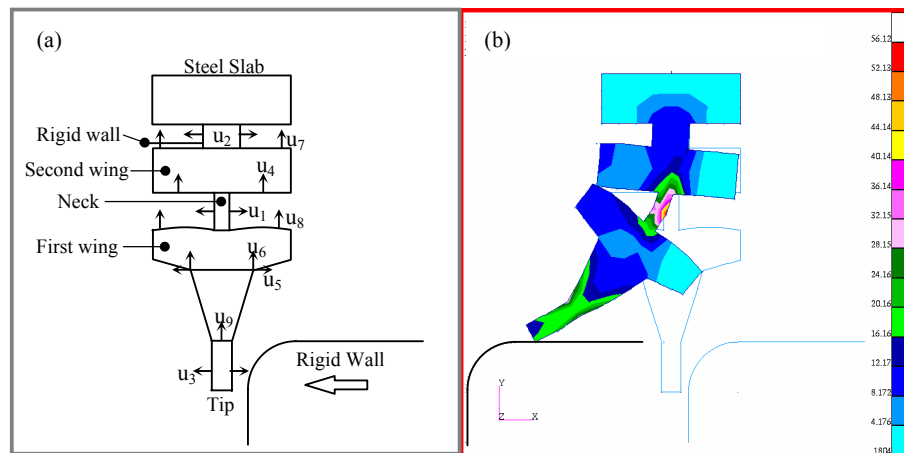


Figure 4. (a) Windshield blade geometry and shape design variables, (b) Contour plot of equivalent stress.

first by perturbing the boundary curve corresponding to the design variable, and the domain design velocity field is computed using an isoparametric mapping method. Four performance measures are chosen: the total area of the structure, two von Mises stresses of the neck region, and the contact force at the tip.

Sensitivity analysis is carried out at each converged load step to compute the material derivative of the displacement. The sensitivities of the performance measures are computed at the final converged load step using \dot{z} . The cost of the sensitivity computation is about 4% of that of the response analysis per design variable, which is quite efficient compared to the finite difference method. The accuracy of the sensitivity is compared with the forward finite difference results for the perturbation size of $\tau = 10^{-6}$. Table 1 shows the accuracy of the sensitivity results. In the third column of Table 1, $\Delta\psi$ denotes the finite difference results and the fourth column represents the change of the function from the proposed method. Excellent sensitivity results are obtained.

Table 1. Sensitivity results and comparison with finite difference method

Design	ψ	$\Delta\psi$	$\dot{\psi}$	$(\Delta\psi / \dot{\psi})\%$
1	Area	.28406E-5	.28406E-5	100.00
	$\sigma_{VM}(53)$.19984E-3	.19984E-3	100.00
	$\sigma_{VM}(54)$.28588E-3	.28588E-3	100.00
	F_C	.55399E-5	.55399E-5	100.00
3	Area	.68663E-5	.68663E-5	100.00
	$\sigma_{VM}(53)$.19410E-3	.19410E-3	100.00
	$\sigma_{VM}(54)$.68832E-4	.68832E-4	100.00
	F_C	.43976E-4	.43976E-4	100.00

5.2. Design Sensitivity Analysis of the Deepdrawing Problem⁵⁴

Figure 5(a) shows the simulation setting and the design variables of the problem. Only half of the model is solved using symmetric conditions. A total of 303 RKPM particles are used to model the blank with elastoplastic material. The punch, draw die, and blank holder are assumed to be rigid bodies, modeled as piecewise linear segments. The draw die is fixed during the punch motion stage, while the blank holder supports force to prevent vertical motion of the blank. After the punch moves to the maximum down-stroke (30 mm), the blank is released to calculate springback. Six design variables are defined, including the horizontal and vertical position of the punch, corner radii of the punch and draw die, the thickness of the blank, and the gap between the blank holder and the die.

Figure 5(b) provides a contour plot of effective plastic strain after springback. A significant amount of sliding is observed between the workpiece and the draw die. High plastic strain distribution is observed in the vertical section. In the optimization, the maximum allowable amount of plastic strain is limited to prevent material failure due to excessive plastic deformation.

Two different types of results are evaluated: the amount of springback and effective plastic strain e_p . The amount of springback is defined as a difference between deformations at the maximum down-stroke and after releasing the blank. Since the sensitivity of effective plastic strain is updated at each load step, no additional computation is required for e_p . The sensitivity of the springback is calculated using the displacement sensitivity.

The accuracy of sensitivity result is compared with the finite difference result by slightly perturbing the design and re-solving the same problem. Table 2 compares the accuracy of the proposed sensitivity $\dot{\psi}$ with the finite difference result $\Delta\psi$. A very good agreement between two methods is observed. A perturbation of $\tau = 10^{-6}$ is used for the finite difference results. In this example, it is hard to find an appropriate perturbation size because the sensitivity

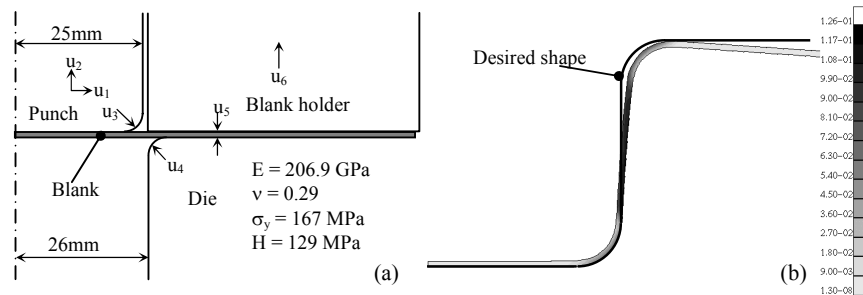


Figure 5. (a) Geometry of the deepdrawing problem and design variables. (b) Effective strain plot after springback. The solid line is the deformed geometry at the maximum down-stroke.

Table 2. Sensitivity results and comparison with finite difference method

Design	ψ	$\Delta\psi$	$\dot{\psi}$	$(\Delta\psi / \dot{\psi})\%$
1	springback	-4.31897E-5	-4.37835E-5	98.64
	$e_p(41)$	1.48092E-8	1.48111E-8	99.99
	$e_p(55)$	2.92573E-8	2.92558E-8	100.01
	$e_p(157)$	-2.08880E-8	-2.08875E-8	100.00
3	springback	1.50596E-5	1.55745E-5	96.69
	$e_p(41)$	-1.81265E-9	-1.81292E-9	99.99
	$e_p(55)$	-1.60858E-8	-1.60891E-8	99.98
	$e_p(157)$	1.14224E-8	1.14229E-8	99.99

magnitudes of the two functions are very different.

The computational cost of the sensitivity analysis is 3.8% of the analysis cost per design variable. Such efficiency is to be expected, since sensitivity analysis uses the decomposed tangent stiffness matrix, and no iteration is required.

5. Conclusions and Outlook

The design sensitivity formulations for various nonlinear problems are presented, including nonlinear elasticity, small and large deformation elastoplasticity, and frictionless contact problems. Even if the structural analysis contains combined nonlinearities, the consistent derivative yields very accurate sensitivity results. One of the most important advantages of the proposed approach is the computational efficiency of calculating sensitivity information, which is critical in the gradient-based optimization. Due to the facts that the proposed approach does not require iteration and uses the decomposed stiffness matrix from the structural analysis, it is shown through numerical examples that the computational cost of the sensitivity calculation is less than 5% of the analysis cost.

References

- 1 K.-J. Bathe, *Finite Element Procedures in Engineering Analysis* (Prentice-Hall, Englewood Cliffs, New Jersey, 1996).
- 2 D. Y. Yang, T. J. Kim, and S. J. Yoon, Proc. In. Mech. Eng., Part B: J. Eng. Manufact. **217**, 1553 (2003).
- 3 K. K. Choi and N. H. Kim, *Structural Sensitivity Analysis and Optimization 1: Linear Systems* (Springer, New York, 2004).
- 4 K. K. Choi and N. H. Kim, *Structural Sensitivity Analysis and Optimization 2: Nonlinear Systems and Applications* (Springer, New York, 2004).
- 5 J. Cea, in *Optimization of Distributed Parameter Structures; Vol. 2*, Ed. E. J. Haug and J. Cea (Sijthoff & Noordhoff, Alphen aan den Rijn, The Netherlands, 1981), p. 1005.
- 6 R. T. Haftka, AIAA J. **20**, 1765 (1982).
- 7 C.-J. Chen and K. K. Choi, AIAA J. **32**, 2099 (1994).
- 8 R. T. Haftka and D. S. Malkus, Int. J. Numer. Methods Eng. **17**, 1811 (1981).
- 9 C. H. Tseng and J. S. Arora, AIAA J. **27**, 117 (1989).
- 10 K. K. Choi and E. J. Haug, J. Struct. Mech. **11**, 231 (1983).
- 11 J. S. Arora, T.-H. Lee, and J. B. Cardoso, AIAA J. **30**, 1638 (1992).
- 12 D. G. Phelan and R. B. Haber, Comp. Meth. Appl. Mech. Eng. **77**, 31 (1989).
- 13 G. D. Pollock and A. K. Noor, Comp. Struct. **61**, 251 (1996).
- 14 S. Kibsgaard, Int. J. Numer. Methods Eng. **34**, 901 (1992).
- 15 N. Olhoff, J. Rasmussen, and E. Lund, Struct. Multidiscipl. Optim. **21**, 1 (1993).
- 16 L. B. Rall and G. F. Corliss, in *Computational Differentiation: Techniques, Applications, and Tools* (1996), p. 1.

- 17 I. Ozaki and T. Terano, *Finite Elem. Anal. Design* **14**, 143 (1993).
- 18 J. Borggaard and A. Verma, *SIAM J. Sci. Comp.* **22**, 39 (2000).
- 19 F. van Keulen, R. T. Haftka, and N. H. Kim, *Comp. Meth. Appl. Mech. Eng.* **194**, 3213 (2005).
- 20 E. J. Haug, K. K. Choi, and V. Komkov, *Design Sensitivity Analysis of Structural Systems* (Academic Press, London, 1986).
- 21 N. H. Kim, K. K. Choi, J. S. Chen, and Y. H. Park, *Comp. Mech.* **25**, 157 (2000).
- 22 N. H. Kim, K. K. Choi, and J. S. Chen, *AIAA J.* **38**, 1742 (2000).
- 23 N. H. Kim, K. K. Choi, and J. S. Chen, *Comp. Struct.* **79**, 1959 (2001).
- 24 N. H. Kim, Y. H. Park, and K. K. Choi, *Struct. Multidiscipl. Optim.* **21**, 196 (2001).
- 25 N. H. Kim, K. K. Choi, J. S. Chen, and M. E. Botkin, *Mech. Struct. Machines* **53**, 2087 (2002).
- 26 N. H. Kim and K. K. Choi, *Mech. Struct. Machines* **29**, 351 (2002).
- 27 N. H. Kim, K. K. Choi, and M. Botkin, *Struct. Multidiscipl. Optim.* **24**, 418 (2003).
- 28 N. H. Kim, K. Yi, and K. K. Choi, *Int. J. Solids and Struct.* **39**, 2087 (2002).
- 29 N. H. Kim, K. K. Choi, and J. S. Chen, *Mech. Struct. Machines* **51**, 1385 (2001).
- 30 K. Schweizerhof and E. Ramm, *Comp. Struct.* **18**, 1099 (1984).
- 31 S. Badrinarayanan and N. Zabaras, *Comp. Meth. Appl. Mech. Eng.* **129**, 319 (1996).
- 32 J. L. T. Santos and K. K. Choi, *Struct. Multidiscipl. Optim.* **4**, 23 (1992).
- 33 K. K. Choi and W. Duan, *Int. J. Numer. Methods Eng.* (2000).
- 34 I. Grindeanu, K. H. Chang, K. K. Choi, and J. S. Chen, *AIAA J.* **36**, 618 (1998).
- 35 Y. H. Park and K. K. Choi, *Mech. Struct. Machines* **24**, 217 (1996).
- 36 T. Belytschko, W. K. Liu, and B. Moran, *Nonlinear Finite Elements for Continua and Structures* (Wiley, New York, 2001).
- 37 J. C. Simo and R. L. Taylor, *Comp. Meth. Appl. Mech. Eng.* **85**, 273 (1991).
- 38 S. Cho and K. K. Choi, *Int. J. Numer. Methods Eng.* **48**, 375 (2000).
- 39 G. Bueda, L. Gil, and E. Onate, *Struct. Multidiscipl. Optim.* **17**, 162 (1999).
- 40 M. Kleiber, *Comp. Meth. Appl. Mech. Eng.* **108**, 73 (1993).
- 41 M. Ohsaki and J. S. Arora, *Int. J. Numer. Methods Eng.* **37**, 737 (1994).
- 42 E. Rohan and J. R. Whiteman, *Comp. Meth. Appl. Mech. Eng.* **187**, 261 (2000).
- 43 C. A. Vidal and R. B. Haber, *Comp. Meth. Appl. Mech. Eng.* **107**, 393 (1993).
- 44 J. C. Simo and R. L. Taylor, *Comp. Meth. Appl. Mech. Eng.* **48**, 101 (1985).
- 45 E. H. Lee, *J.f Appl Mech* **36**, 1 (1969).
- 46 J. C. Simo, *Comp. Meth. Appl. Mech. Eng.* **99**, 61 (1992).
- 47 P. Wriggers, T. V. Van, and E. Stein, *Comp. Struct.* **37**, 319 (1990).
- 48 T. A. Laursen and J. C. Simo, *Int. J. Numer. Methods Eng.* **36**, 2451 (1993).
- 49 N. Kikuchi and J. T. Oden, *Contact Problems in Elasticity: a Study of Variational Inequalities and Finite Element Method* (SIAM, Philadelphia, VA, 1988).
- 50 J. Sokolowski and J. P. Zolesio, *Introduction to Shape Optimization* (Springer-Verlag, Berlin, 1991).
- 51 A. Haraux, *J. Math. Soc. Japan* **29**, 615 (1977).
- 52 W. K. Liu, S. Jun, and Y. F. Zhang, *Int. J. Numer. Methods Eng.* **20**, 1081 (1995).
- 53 J. S. Chen, C. T. Wu, S. Yoon, and Y. You, *Int. J. Numer. Methods Eng.* **50**, 435 (2001).
- 54 K. K. Choi and N. H. Kim, *AIAA J.* **40**, 147 (2002).